ACS APPLIED MATERIALS & INTERFACES

Research Article

www.acsami.org

Flexible Binder-Free Metal Fibril Mat-Supported Silicon Anode for High-Performance Lithium-Ion Batteries

Seonghyun Song,[†,§] Sang Woo Kim,[‡,§] Dong Jin Lee,[∥] Young-Gi Lee,[⊥] Kwang Man Kim,[⊥] Chang-Hyeon Kim,[#] Jung-Ki Park,[∥] Yong Min Lee,*[,†] and Kuk Young Cho*[,‡]

[†]Department of Chemical & Biological Engineering, Hanbat National University, 125 Dongseodaero, Yuseong-gu, Daejeon, 305-719, Republic of Korea

[‡]Division of Advanced Materials Engineering, Kongju National University, 1223-24 Cheonan-daero, Cheonan, Chungnam 331-717, Republic of Korea

[∥]Department of Chemical and Biomolecular Engineering, Korea Advanced Institute of Science and Technology (KAIST), Daejeon, 305-701, Republic of Korea

[⊥]Power Control Device Research Team, Electronics and Telecommunications Research Institute (ETRI), 218, Gajeongno, Yuseong-gu, Daejeon, 305-700, Republic of Korea

[#]Shine Company Limited, 192-12, Busan, 614-865, Republic of Korea

Supporting Information

ABSTRACT: We report the fabrication of a flexible and binder-free metal fibril mat-supported Si anode (Si@SFM) by a simple process. The fabricated Si@SFM anode showed a high discharge capacity, ~3000 mAh g^{-1} at a current rate of 300 mA g^{-1}, and exhibited stable capacity retention, 90% at a 1 C rate (2000 mA g^{-1}) after 200 cycles. The rate capability of the electrode was still high even when both the charge and the discharge current rates were markedly increased at the same time (1234 mAh g^{-1} for charge−discharge time of ~12 min). Moreover, owing to its mechanical flexibility, the Si@SFM can be adopted as a key component of flexible lithium-ion batteries (LIBs). After cell packaging, the rechargeable flexible battery under bending stress showed only a little capacity fading (86% of initial capacity) at 1000 mA g^{-1} over 150 cycles. These results suggest that the Si@SFM electrode is readily suitable for use in rechargeable flexible LIBs.

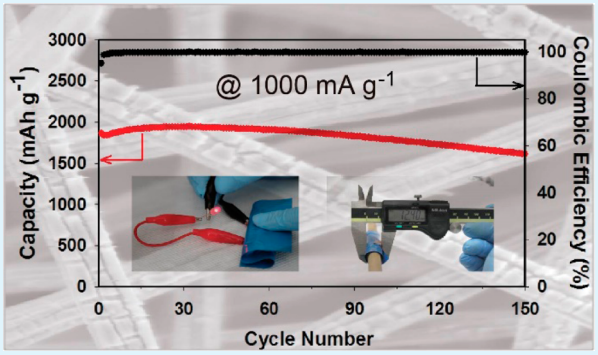

KEYWORDS: *silicon anode, binder-free anode, metal fibril, magnetron sputtering, flexible Li-ion battery*

1. INTRODUCTION

As interest in flexible electronic devices, such as flexible liquid crystalline displays (LCDs), organic light-emitting diodes (OLEDs), wearable computers, and medical devices, grows, development of flexible power sources, including lithium batteries, supercapacitors, and solar cells, has become an important goal.[1−6] Of these, rechargeable lithium-ion batteries (LIBs) are particularly attractive owing to their wide commercial use in mobile electronic devices given their high energy densities.[7−9] However, research on flexible LIBs is still in the nascent stage; numerous challenges remain to be overcome, and a number of phenomena remain unexplored. Thus, it is important to consider the major differences between conventional, rigid power sources and flexible ones.[6,10] To begin with, flexible power sources should be able to withstand mechanical stresses originating from external physical deformation, that is, the materials used to fabricate the flexible batteries should also exhibit flexibility. The primary components of LIBs are the electrodes fabricated by coating with active materials, a binder, and a conducting agent in slurry form on a metallic foil as a current collector. Cu foil is used for the anode and Al foil for the cathode.[11] Such conventionally fabricated electrodes are quite rigid against external bending or rolling deformations. Their poor mechanical flexibility limits their use in flexible LIBs. Carbon-based films[12−14] and conducting polymers[15,16] have been proposed as alternatives for fabricating mechanically flexible electrodes. However, they exhibit low electric conductivities compared to pure metallic foils, resulting in relatively poor electrochemical performance. Recent reports suggest that novel thin metallic layers deposited on porous membranes not only exhibit the desired flexibility when used as electrodes but also can act as templates for nanostructures that allow use of high-energy-capacity silicon (Si) anodes in the form of thin layers.[17] This indicates that flexible current collectors made from metallic materials should be used to form

Received: April 14, 2014
Accepted: July 8, 2014
Published: July 8, 2014

electrodes for low electrical conductance active materials in flexible LIBs.

Recent research on LIBs has focused on the use of Si as a high capacity anode material, as it can exhibit a theoretical specific capacity that is over 10 times that of graphite.[18−23] Two major drawbacks of Si anodes, however, are the significant volume change (up to 400%) during charge−discharge cycling and their low electrical conductivity.[24−26] Herein, we report the fabrication of a binder-free metal fibril mat-supported Si (Si@SFM) anode by a one-step process using a sputtering method. The Si@SFM anode possesses desirable LIB properties owing to its uniform deposition and its interconnected structure. The Si@SFM readily permits facile Li-ion and electron transport and also accommodates large volume changes of Si.[21,26,27] Moreover, we tested the suitability of the anode for use in flexible LIBs by characterizing the electrochemical performances of flexible cells based on a Si@SFM anode, which had high mechanical flexibility and electrical conductivity.

2. EXPERIMENTAL SECTION

Fabrication of the Si@SFM anode was carried out using the radiofrequency (RF) magnetron sputtering method. The base vacuum pressure of the stainless-steel chamber was 2.0×10^{-5} Torr, and the working pressure was 7.0×10^{-3} Torr of Ar (99.999%). The Si target (99.99%, Tasco) was used, and the distance between target and substrate was 7 cm. Before Si was deposited on the stainless steel fibril mat (SFM) current collectors (thickness, 100 μm; areal density, 10 mg cm^{-2}; surface area, 0.05 m^2 g^{-1}, Sfelt, Shine Co. Ltd.), the Si target was presputtered for 60 min at 50 W to remove the contaminants on its surface. The sputtering was performed for 2 h at 25 °C and 50 W on one side of the SFM. Si was also sputtered on a piece of copper foil (Si@Cu), and the electrode was used for comparison purposes; deposition conditions were the same as those for the Si@SFM electrodes. The surface and cross-sectional morphologies of the samples were examined using a field emission scanning electron microscopy (MIRA LMH, Tescan and FE-SEM, S4800, Hitachi) equipped with an energy-dispersive X-ray spectroscopy (EDX) detector (GENESIS XM2, EDAX Inc.). In order to observe the cross-sectional morphology of the Si@SFM electrode, we cut it using an argon-ion beam polisher (E3500, Hitachi) at a constant power of 2.1 W (6 kV and 0.35 mA) under vacuum (<2.0×10^{-4} Pa).

To evaluate the basic electrochemical properties, 2032 coin-type half-cells were prepared by assembling the electrodes (Si@SFM or Si@Cu), Li metal, and polyethylene (PE) separator (ND420, Asahi-Kasai E-Materials) that was soaked with the liquid electrolyte (1.15 M $LiPF_6$ in EC/EMC (30/70 by vol %)) containing 5 wt % fluoroethylene carbonate (FEC, PANAX ETEC) in an Ar-filled glovebox. The loading density of the active material, Si, was 0.2 mg cm^{-2}. Since the areal density of SFM is 10 mg cm^{-2}, the mass ratio of Si to SFM is around 1:50. The specific capacity (mAh g^{-1}) of cells was calculated based on the sputtered Si mass only. In addition, pouch-type cells (electrode dimension 4 cm × 4 cm) consisting of the Si@SFM electrode, the PE separator soaked with the above-mentioned electrolyte, and Li metal for analyses of flexible battery were fabricated in the glovebox. Full cells using a Si@SFM anode, PE separator soaked with the same electrolyte, and a $LiFePO_4$ cathode ($LiFePO_4$/polyvinylidene fluoride/Super-P = 90/5/5 by wt %) were fabricated to evaluate the suitability of the Si@SFM anode when paired with conventional cathode materials in LIBs. The $LiFePO_4$ cathode was prepared by casting the slurry consisting of $LiFePO_4$ active materials (Life Power P2, Sud-Chemie), polyvinylidene fluoride (KF-1300) binder, and Super-P (Timcal) conductor in *N*-methyl-2-pyrrolidone solvent and followed by drying in an oven at 100 °C. The prepared $LiFePO_4$ electrode has a thickness of 40 μm, a density of 2.0 g cm^{-3}, and a capacity of 0.65 mAh cm^{-2}. The assembled unit cells were cycled at constant current rates ranging from 300 to 12 000 mA g^{-1} over potentials of 0.01−1.5 (vs Li/Li^+) (in the case of the half-cells) and 2.0−4.2 V (vs Li/Li^+) (in the case of the full-cells). A battery tester (PEBC050.1, PNE Solutions) was employed for the purpose, and measurements were performed at 25 °C. Electrochemical impedance spectroscopy (EIS) measurements were conducted using the impedance analyzer (Biologic, VSP) over frequencies ranging from 0.05 Hz to 1 MHz at a potential of 10 mV.

3. RESULTS AND DISCUSSIONS

The surface and cross-sectional morphologies of pristine SFM and Si@SFM electrode materials were characterized by scanning electron microscopy (SEM). The stainless steel fibrils had a diameter of approximately 10 μm and formed an interconnected mat-like structure (Figure 1). An SFM as a current collector allows for fast electron transfer over the entire anode. In addition, the open spaces between neighboring fibrils improve electrolyte diffusion, resulting in higher ion-transfer rates. Thus, it was expected that the fibril mat would improve the electrochemical performance of LIBs when used to form electrodes. Even though the Si@SFM electrode was fabricated by radiofrequency (RF) magnetron sputtering of Si onto the SFM, the coating process did not modify the interconnected structure of the SFM (Figure 1c). The surfaces of the stainless steel fibril were observed to have become smoother after being coated with Si (Figure 1d). The presence of Si on the surface of the stainless steel fibril was also confirmed by the EDX (energy-dispersive X-ray spectroscopy) image shown in Figure 1e. The thickness of the coated Si active layer was determined from cross-sectional images of a single fibril in Si@SFM (Figure 1f). Repeated measurements suggested that a Si coating approximately 1 μm in thickness was formed after 120 min of sputtering corresponding to a growth rate of ~8 nm min^{-1}.

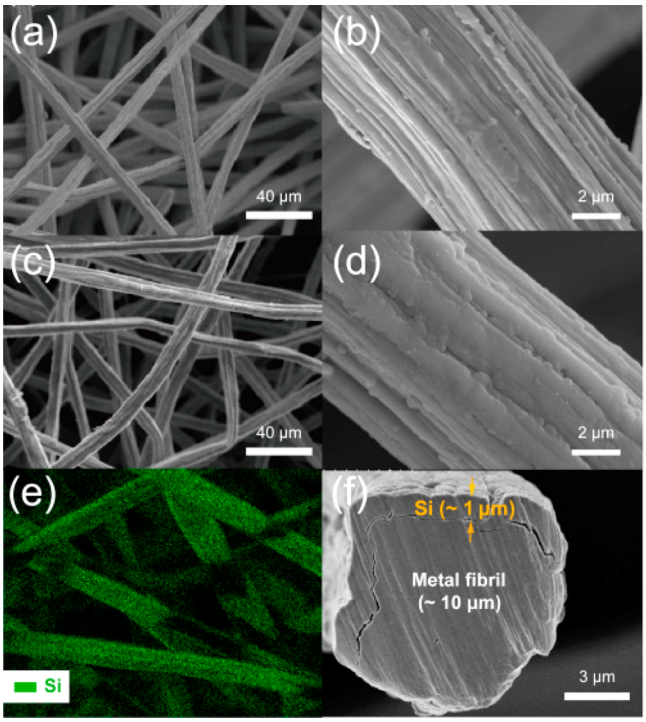

Figure 1. (a and b) SEM images of the pristine nonwoven-shaped 3D stainless steel fibril mats (SFM). (c and d) SEM images of the Si sputtered onto the SFM (Si@SFM). (e) EDX image of the Si (green) coating on the surface of the Si@SFM anode. (f) Cross-sectional SEM image of a single fibril of the Si@SFM anode.

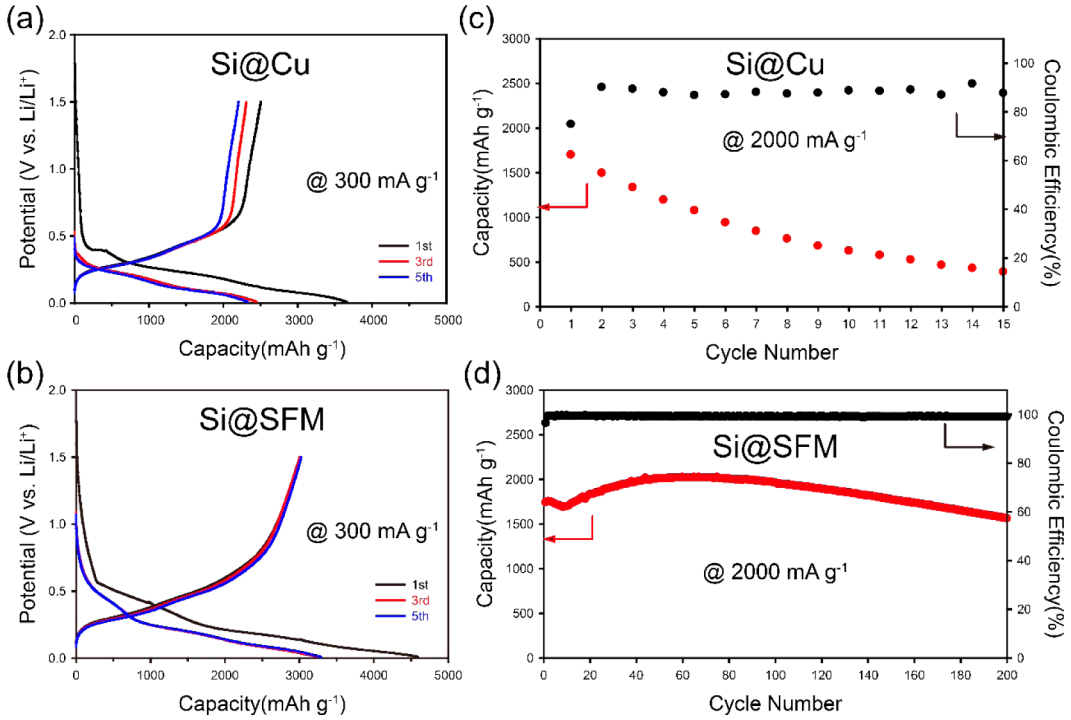

Figure 2. (a and b) Voltage profiles at the 1st, 3rd, and 5th cycle of 2032 coin-type half-cells based on Si@Cu and Si@SFM, respectively, at a current rate of 300 mA g^{-1}. (c and d) Cycle performance of a 2032 coin-type half-cell having Si@Cu and Si@SFM at a high current rate of 2000 mA g^{-1}.

The electrochemical properties of Si@SFM electrodes were investigated using 2032 coin-type half-cells. As noted elsewhere,[17,21] these cells generally employ Li metal as the reference and counter electrode. In addition, a control cell fabricated using Si@Cu was also investigated (with the other fabrication conditions the same as for the Si@SFM cell). Its performance was compared to that of a Si@SFM cell in order to elucidate the effects of the 3D SFM current collector on cell performance (Figure 2 and Figure S1, Supporting Information). The voltage profiles of the unit cells with the Si@Cu and Si@SFM anodes, which were determined at a current rate of 300 mA g^{-1} over potentials ranging from 0.01 to 1.5 V (vs Li/Li^+), are shown in Figure 2a and 2b, respectively. Both cells exhibited typical characteristic voltage profiles associated with the lithiation and delithiation of Si. These results were consistent with the results of previous studies on Si-based anode materials.[28,29] The initial discharge capacities of Si@SFM and Si@Cu cells were 3025 and 2505 mAh g^{-1}, respectively, which indicates that Si@SFM is more electrochemically active under the same Si loading level. The initial Coulombic efficiencies (ICEs) of the cells were 65.8% and 68.4%, respectively. The fact that the ICE of the Si@SFM cell was lower than for Si@Cu can be attributed to the fact that the surface area of the Si@SFM electrode was greater than for the Si@Cu electrode. However, the Coulombic efficiency (CE) of the Si@SFM cell reached 93% after 3 cycles and maintained its value until the end of the preconditioning cycling experiment (the first 5 cycles).

As expected, the interconnected and porous structure of the SFM current collector is readily penetrated by Li ions and also facilitates transportation of electrons. As a result, the Si@SFM electrode exhibited a higher initial discharge capacity than that of the Si@Cu electrode, even at a current density as low as 300 mA g^{-1}. The cycling performances of the Si@SFM and Si@Cu cells were measured at a higher rate, 2000 mA g^{-1}, which is a 1 C rate. The Si@SFM cell exhibited stable cycling performance (its capacity was greater than 1500 mAh g^{-1}) even at the high C rate (Figure 2c and 2d). In contrast, the Si@Cu cell exhibited rapid capacity fading after only 15 cycles (its capacity after 15 cycles, 390 mAh g^{-1}, was only 23% of its initial capacity) at the 1 C rate. This was owing to the relatively thick Si film of the Si@Cu electrode. It is likely that the lack of free volume in the Si@Cu electrodes caused the Si film to be pulverized and peel off from the Cu foil current collector (Figure S1c, Supporting Information). This is likely to be the main cause of the inferior capacity retention and poor CE of Si@Cu electrodes. This result indicates that Si@Cu electrodes consisting of a thick Si film on planar Cu foil are not suited for use as anodes in LIBs. In contrast, the Si@SFM cell exhibited a discharge capacity of 1739 mAh g^{-1}, retaining 90% of its initial discharge capacity after 200 cycles. Moreover, its average CE was greater than 99% for up to 200 cycles.

The Si@SFM cell also demonstrated excellent rate capabilities at current densities ranging from 1000 to 12 000 mA g^{-1} (Figure 3). Even when the charge−discharge current rate was increased by a factor of 12, from 1000 to 12 000 mA g^{-1}, the rate capability of the cell remained as high as 1234 mAh g^{-1} for a charge−discharge time as short as ∼12 min. In addition, as the current density recovered to 1000 mA g^{-1}, the cell capacity was maintained at 94.3% (2571 mAh g^{-1}) based on its original capacity. The superior electrochemical characteristics exhibited by the Si@SFM cell, including a high reversible capacity, excellent cycling performance, high efficiencies during prolonged cycling, and a high rate capability, are all evidence of the positive effects of the open porous and interconnected SFM current collector on LIB performance.[30−32]

In order to analyze the changes in morphology of the Si@SFM electrodes after 200 charge−discharge cycles, the unit cells were disassembled and the electrodes washed with dimethylene carbonate (DMC) to remove residual electrolyte,

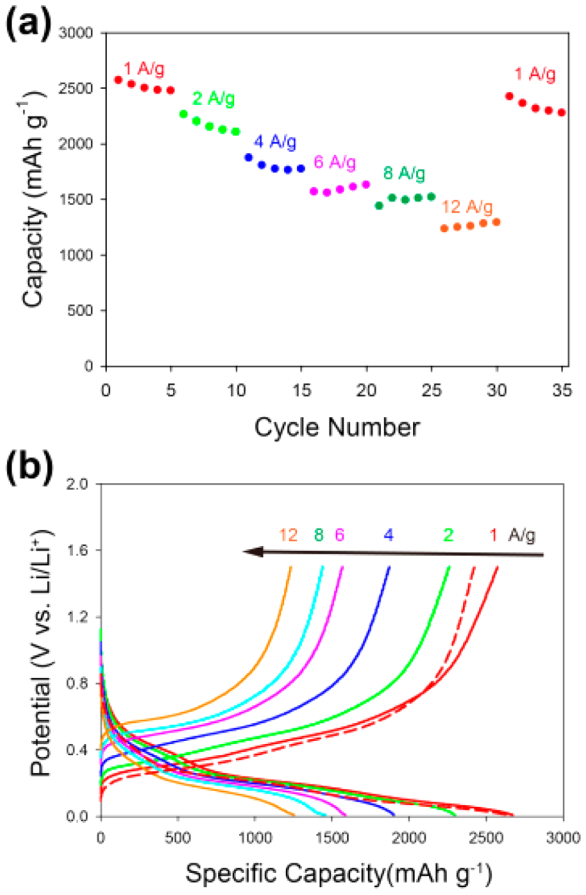

Figure 3. (a and b) Rate capability characteristics of the half-cells based on the Si@SFM anode for different charging and discharging current rates: (dotted line) voltage profile at 1 A g^{-1} rate after the 12 A g^{-1} cycling.

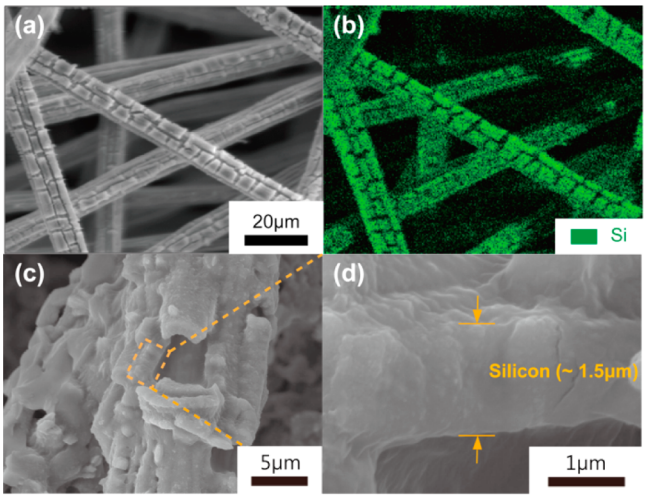

Figure 4. (a) Surface morphology of the Si@SFM after 200 charge–discharge cycles. (b) EDX image of a. (c) Image of Si layer on single fibril. (d) Amplified image of Si layer showing the increased thickness of Si after 200 cycles.

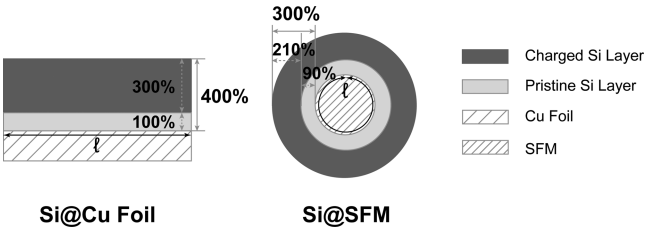

Figure 5. Schematics illustrating the different manner in which the volumes of the planar and the cylindrical Si anodes change.

dried in a vacuum chamber for 24 h, and then imaged. It was found from the surface morphology of the Si@SFM and the corresponding EDX image that Si layer adhered well to the surfaces of the stainless steel fibrils despite evident crack generation (Figure 4a and 4b) and a 50% thickness increase from 1 to 1.5 μm (Figure 4c and 4d). It should be noted the 3D Si@SFM structure suppressed peeling of the thick Si layer during electrochemical cycling, in contrast to what is generally observed in the case of cycled Si@Cu film anode (Figure S1c, Supporting Information).[29,33]

This remarkable improved adhesion property of the Si layer on the stainless steel fibril could be explained by a different geometric expansion mechanism during charging. The lithium intercalation-related volume expansion of a Si layer coated on a flat 2D surface probably occurs in only one direction, leading to severe stress generation. In contrast, the volume of the Si layer coated on the stainless fibrils changed in a radial direction, lowering the stress. For example, as schematically presented in Figure 5, Si on the planar foil current collector can expand by 300% if the coating thickness of Si is assumed to be 100%. However, as for fibril-based current collector, only 90% thickness of Si is needed to coat the same Si loading amount. In addition, the expansion ratio could be suppressed by around 210%. This might be the reason for the well-adhered Si layer, despite the evident crack formation. Excellent cycling performance of the Si@SFM cell compared to that of the Si@Cu cell also reflected advantages of the Si@SFM electrode structure.

Owing to the mechanical flexibility and high electrical conductivity of the SFM substrate (Figure S2, Supporting Information), application of Si@SFM electrodes could be extended to next-generation flexible batteries. The suitability of the Si@SFM anode for use in flexible LIBs was determined using a pouch-type cell (dimension of electrode = 4 cm × 4 cm, see Figure S3, Supporting Information). To examine the flexibility of the LIB cell, we investigated whether the pouch-type cell with the Si@SFM electrode could light up a red LED when folded (Figure S4a, Supporting Information). To further evaluate the electrochemical performance of the cell under mechanical stress, it was rolled with a bending radius of 0.6 cm (Figure S4b, Supporting Information) and cycled at a current rate of 0.5 C (1000 mA g^{-1}). The flexible cell exhibited a discharge capacity of 1616 mAh g^{-1} as shown in Figure 6. Interestingly, its average CE was greater than 99% for up to 150 cycles. This implies that the mechanical flexibility and high electrical conductivity of the SFM current collector allows it to act as a pathway for electrons (with the interfibrillar pores remaining open) even when rolled or subjected to bending stress. Finally, we fabricated a flexible full cell using the Si@SFM anode and a $LiFePO_4$ cathode and evaluated it for cell performance.[32] Even though the cell design parameters and conditions (i.e., the electrode area ratio and the negative/positive capacity ratio, or N/P ratio) were not optimized, the full cell exhibited very stable capacity retention behavior at a current rate of 1 C over 50 cycles, retaining 76% of its initial capacity (Figure 7). When the full cell capacity is converted into a Si-based value, it reaches 1300 mAh g^{-1} at a current rate

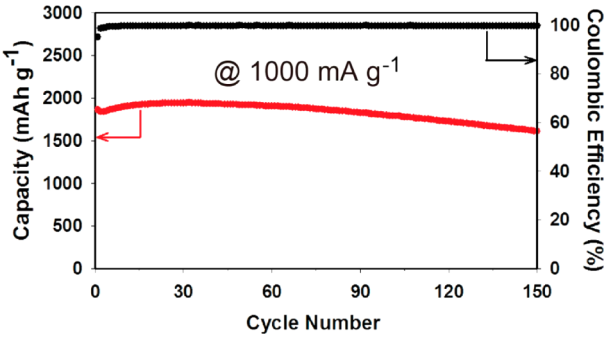

Figure 6. Cycle performance of the flexible Si@SFM pouch cell (bending radius = 0.6 cm) as a function of cycle number at a high current rate of 1000 mA g^{-1}.

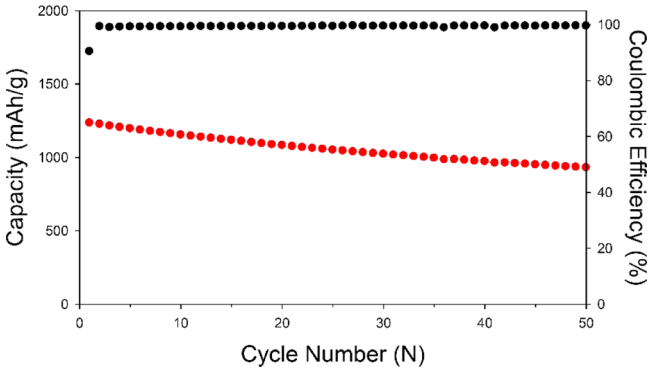

Figure 7. Cycle performances of a flexible full-cell consisting of $LiFePO_4$/Si@SFM (bending radius = 0.6 cm) at a current of 2000 mA g^{-1}.

of 2000 mA g^{-1}. In addition, the average CE of the cell was in the range of 99.2%, indicating good reversibility even under full cell conditions.[3,32] Therefore, the Si@SFM electrode investigated in the present study shows great potential for use in flexible LIBs.

4. CONCLUSION

We successfully fabricated a flexible LIB electrode consisting of a Si coating layer on a 3D stainless steel fibril mat, which acts as a current collector. The resulting Si@SFM electrode showed excellent electrochemical performances both in coin-type and in pouch-type cells, examples of rigid and flexible LIBs, respectively. The high rate capability of the Si@SFM cells was attributable to the 3D open-porous nature of the current collector. Our approach of using a flexible 3D-structured metallic mat as the current collector should aid development of high energy density flexible LIBs.

■ ASSOCIATED CONTENT

Supporting Information

Voltage profiles of Si@Cu foil and Si@SFM half-cells, electrochemical impedance spectroscopy of the Si@Cu foil and Si@SFM, SEM images of Si@Cu; schematic and photographs of the flexible Si@SFM anode; photoimage of pristine SFM and Si-sputtered Si@SFM ultrasonically welded with Cu lead tabs; lighting an LED from the S-curve bent Si@SFM pouch cell and rolling condition of the flexible Si@SFM pouch cell for cycling tests. This material is available free of charge via the Internet at http://pubs.acs.org.

■ AUTHOR INFORMATION

Corresponding Authors

*E-mail: yongmin.lee@hanbat.ac.kr (Y.M.L.).
*E-mail: kycho@kongju.ac.kr (K.Y.C.).

Author Contributions

§These authors contributed equally to this work.

Notes

The authors declare no competing financial interest.

■ ACKNOWLEDGMENTS

This research was supported by the Converging Research Centre Program through the Ministry of Science, ICT and Future Planning, Korea (2013K000288) and Chungcheong Leading Industry Promotion Project of the Korean Ministry of Trade, Industry and Energy.

■ REFERENCES

(1) Nishide, H.; Oyaizu, K. Toward Flexible Batteries. *Science* **2008**, *319*, 737−738.
(2) Miller, J. R. Valuing Reversible Energy Storage. *Science* **2012**, *335*, 1312−1313.
(3) Hu, L.; Wu, H.; La Mantia, F.; Yang, Y.; Cui, Y. Thin, Flexible Secondary Li-Ion Paper Batteries. *ACS Nano* **2010**, *4*, 5843−5848.
(4) Liu, B.; Zhang, J.; Wang, X.; Chen, G.; Chen, D.; Zhou, C.; Shen, G. Hierarchical Three-Dimensional $ZnCo_2O_4$ Nanowire Arrays/Carbon Cloth Anodes for a Novel Class of High-Performance Flexible Lithium-Ion Batteries. *Nano Lett.* **2012**, *12*, 3005−3011.
(5) Chen, Y.; Au, J.; Kazlas, P.; Ritenour, A.; Gates, H.; McCreary, M. Flexible Active Matrix Electronic ink display. *Nature* **2003**, *423*, 136.
(6) Li, N.; Chen, Z.; Ren, W.; Li, F.; Cheng, H. M. Flexible Graphene-based Lithium Ion Batteries With Ultrafast Charge and Discharge Rates. *Proc. Natl. Acad. Sci. U.S.A.* **2012**, *109*, 17360−17365.
(7) Scrosati, B. Challenge of Portable Power. *Nature* **1995**, *373*, 557−558.
(8) Jeong, G.; Kim, Y. U.; Kim, H.; Kim, Y. J.; Sohn, H. J. Prospective Materials and Applications for Li Secondary Batteries. *Energy Environ. Sci.* **2011**, *4*, 1986−2002.
(9) Pushparaj, V. L.; Shaijumon, M. M.; Kumar, A.; Murugesan, S.; Ci, L.; Vajtai, R.; Linhardt, R. J.; Nalamasu, O.; Ajayan, P. M. Flexible Energy Storage Devices Based on Nanocomposite Paper. *Proc. Natl. Acad. Sci. U.S.A.* **2007**, *104*, 13574−13577.
(10) Yun, J. H.; Han, G. B.; Lee, Y. M.; Lee, Y. G.; Kim, K. M.; Park, J. K.; Cho, K. Y. Low Resistance Flexible Current Collector for Lithium Secondary Battery. *Electrochem. Solid-State Lett.* **2011**, *14*, A116−A119.
(11) Tarascon, J. M.; Armand, M. Issues and Challenges Facing Rechargeable Lithium Batteries. *Nature* **2001**, *414*, 359−367.
(12) Zhou, G.; Wang, D.-W.; Hou, P.-X.; Li, W.; Li, N.; Liu, C.; Li, F.; Cheng, H.-M. A Nanosized Fe_2O_3 Decorated Single-walled Carbon Nanotube Membrane as a High-Performance Flexible Anode for Lithium Ion Batteries. *J. Mater. Chem.* **2012**, *22*, 17942−17946.
(13) Kobashi, K.; Hirabayashi, T.; Ata, S.; Yamada, T.; Futaba, D. N.; Hata, K. Green, Scalable, Binderless Fabrication of a Single-Walled Carbon Nanotube Nonwoven Fabric Based on an Ancient Japanese Paper Process. *ACS Appl. Mater. Interfaces* **2013**, *5*, 12602−12608.
(14) Hu, L.; Liu, N.; Eskilsson, M.; Zheng, G.; McDonough, J.; Wågberg, L.; Cui, Y. Silicon-conductive Nanopaper for Li-ion Batteries. *Nano Energy* **2013**, *2*, 138−145.
(15) Chen, J.; Liu, Y.; Minett, A. I.; Lynam, C.; Wang, J.; Wallace, G. G. Flexible, Aligned Carbon Nanotube/Conducting Polymer Electrodes for a Lithium-Ion Battery. *Chem. Mater.* **2007**, *19*, 3595−3597.
(16) Nyholm, L.; Nyström, G.; Mihranyan, A.; Strømme, M. Toward Flexible Polymer and Paper-Based Energy Storage Devices. *Adv. Mater.* **2011**, *23*, 3751−3769.
(17) Choi, J.-Y.; Lee, D. J.; Lee, Y. M.; Lee, Y.-G.; Kim, K. M.; Park, J.-K.; Cho, K. Y. Silicon Nanofibrils on a Flexible Current Collector for

Bendable Lithium-Ion Battery Anodes. *Adv. Funct. Mater.* **2013**, *23*, 2108−2114.
(18) Li, X.; Cho, J.-H.; Li, N.; Zhang, Y.; Williams, D.; Dayeh, S. A.; Picraux, S. T. Carbon Nanotube-Enhanced Growth of Silicon Nanowires as an Anode for High-Performance Lithium-Ion Batteries. *Adv. Energy Mater.* **2012**, *2*, 87−93.
(19) Erk, C.; Brezesinski, T.; Sommer, H.; Schneider, R.; Janek, J. Toward Silicon Anodes for Next-Generation Lithium Ion Batteries: A Comparative Performance Study of Various Polymer Binders and Silicon Nanopowders. *ACS Appl. Mater. Interfaces* **2013**, *5*, 7299−7307.
(20) Zhou, M.; Cai, T.; Pu, F.; Chen, H.; Wang, Z.; Zhang, H.; Guan, S. Graphene/Carbon-Coated Si Nanoparticle Hybrids as High-Performance Anode Materials for Li-Ion Batteries. *ACS Appl. Mater. Interfaces* **2013**, *5*, 3449−3455.
(21) Lee, D. J.; Lee, H.; Ryou, M.-H.; Han, G.-B.; Lee, J.-N.; Song, J.; Choi, J.; Cho, K. Y.; Lee, Y. M.; Park, J.-K. Electrospun Three-Dimensional Mesoporous Silicon Nanofibers as an Anode Material for High-Performance Lithium Secondary Batteries. *ACS Appl. Mater. Interfaces* **2013**, *5*, 12005−12010.
(22) Liu, C.; Li, F.; Lai-Peng, M.; Cheng, H. M. Advanced Materials for Energy Storage. *Adv. Mater.* **2010**, *22*, E28−E62.
(23) Dahn, J. R.; Zheng, T.; Liu, Y.; Xue, J. S. Mechanisms for Lithium Insertion in Carbonaceous Materials. *Science* **1995**, *270*, 590−598.
(24) Guo, J.; Chen, X.; Wang, C. Carbon Scaffold Structured Silicon Anodes for Lithium-ion Batteries. *J. Mater. Chem.* **2010**, *20*, 5035−5040.
(25) Lee, D. J.; Ryou, M.-H.; Lee, J.-N.; Kim, B. G.; Lee, Y. M.; Kim, H.-W.; Kong, B.-S.; Park, J.-K.; Choi, J. W. Nitrogen-doped Carbon Coating for a High-performance SiO Anode in Lithium-ion Batteries. *Electrochem. Commun.* **2013**, *34*, 98−101.
(26) Aricò, A. S.; Bruce, P.; Scrosati, B.; Tarascon, J. M.; Van Schalkwijk, W. Nanostructured Materials for Advanced Energy Conversion and Storage Devices. *Nat. Mater.* **2005**, *4*, 366−377.
(27) Wu, H.; Cui, Y. Designing Nanostructured Si Anodes for High Energy Lithium Ion Batteries. *Nano Today* **2012**, *7*, 414−429.
(28) Chan, C. K.; Peng, H.; Liu, G.; McIlwrath, K.; Zhang, X. F.; Huggins, R. A.; Cui, Y. High-performance Lithium Battery Anodes Using Silicon Nanowires. *Nat. Nanotechnol.* **2008**, *3*, 31−35.
(29) Han, G.-B.; Ryou, M.-H.; Cho, K. Y.; Lee, Y. M.; Park, J.-K. Effect of Succinic Anhydride as an Electrolyte Additive on Electrochemical Characteristics of Silicon Thin-film Electrode. *J. Power Sources* **2010**, *195*, 3709−3714.
(30) Teki, R.; Datta, M. K.; Krishnan, R.; Parker, T. C.; Lu, T.-M.; Kumta, P. N.; Koratkar, N. Nanostructured Silicon Anodes for Lithium Ion Rechargeable Batteries. *Small* **2009**, *5*, 2236−2242.
(31) Lee, D. J.; Choi, J.; Ryou, M.-H.; Kim, C.-H.; Lee, Y. M.; Park, J.-K. Binder-free Metal Fibril-supported Fe_2O_3 Anodes for High-performance Lithium-ion Batteries. *J. Mater. Chem. A* **2014**, *2*, 2906−2909.
(32) Cho, G. B.; Song, M. G.; Bae, S. H.; Kim, J. K.; Choi, Y. J.; Ahn, H. J.; Ahn, J. H.; Cho, K. K.; Kim, K. W. Surface-modified Si Thin Film Electrode for Li Ion Batteries ($LiFePO_4$/Si) by Cluster-structured Ni under Layer. *J. Power Sources* **2009**, *189*, 738−742.
(33) Maranchi, J.; Hepp, A.; Evans, A.; Nuhfer, N.; Kumta, P. Interfacial Properties of the a-Si/Cu:Active−Inactive Thin-Film Anode System for Lithium-Ion Batteries. *J. Electrochem. Soc.* **2006**, *153* (6), A1246−A1253.